Celestial Mechanics and Dynamical Astronomy (2021) 133:50
https://doi.org/10.1007/s10569-021-10049-1

ORIGINAL ARTICLE

A generalization of the equinoctial orbital elements

Giulio Baù[1] · Javier Hernando-Ayuso[2] · Claudio Bombardelli[3]

Received: 20 March 2021 / Revised: 15 August 2021 / Accepted: 25 October 2021 /
Published online: 25 November 2021

Abstract
We introduce six quantities that generalize the equinoctial orbital elements when some or all the perturbing forces that act on the propagated body are derived from a potential. Three of the elements define a non-osculating ellipse on the orbital plane, other two fix the orientation of the equinoctial reference frame, and the last allows us to determine the true longitude of the body. The Jacobian matrices of the transformations between the new elements and the position and velocity are explicitly given. As a possible application, we investigate their use in the propagation of Earth's artificial satellites, showing a remarkable improvement compared to the equinoctial orbital elements.

Keywords Non-singular orbital elements · Orbit computation

1 Introduction

The set of elements investigated by Broucke and Cefola (1972):

$$\begin{aligned} &a, && \lambda_0 = M_0 + \omega + \Omega, \\ &h = e\sin(\omega+\Omega), && k = e\cos(\omega+\Omega), \\ &p = \tan\frac{i}{2}\sin\Omega, && q = \tan\frac{i}{2}\cos\Omega, \end{aligned} \tag{1}$$

where a, e, i, Ω, ω, M_0 are the classical Keplerian elements, are usually referred to as the *equinoctial orbital elements*, hereafter EqOE. This expression was coined by Arsenault et al. (1970), who were also the first to introduce the equinoctial reference frame (see Sect. 2.2). The appearance of similar elements in Celestial Mechanics dates back to Lagrange's secular theory of planetary motion. A slight different version of the quantities p, q, where the inclination i replaces $i/2$, is employed in Lagrange (1781, p. 130). Moreover, the two quantities N and

✉ Giulio Baù
giulio.bau@unipi.it

1 University of Pisa, Largo B. Pontecorvo 5, 56127 Pisa, Italy

2 ispace, inc., Sumitomo Fudosan Hamacho Building 3F, 3-42-3, Nihonbashi Hamacho, Chuo-ku, Tokyo 103-0007, Japan

3 Technical University of Madrid (UPM), E-28040 Madrid, Spain

M introduced at p. 135 of Lagrange's paper are a small-inclination approximation of k and h, after dividing by the gravitational parameter.

One of the most relevant variations of the EqOE is due to Walker et al. (1985). They proposed to replace the semi-major axis with the semi-latus rectum and the mean longitude at epoch (λ_0) with the true longitude. In this way, the resulting set can be applicable to all orbits, while the EqOE work with negative values of the Keplerian energy only. However, both sets are singular for retrograde equatorial orbits (i.e., $i = \pi$) and for rectilinear motion. These *modified* equinoctial elements are particularly suitable for optimal low-thrust orbit transfers as described in Kéchichian (2018).

Battin (1999, Sect. 10.4) provided useful relations for the classical equinoctial elements and their time derivatives, employing the mean longitude in place of λ_0. Broucke and Cefola (1972) reported also the matrix of the partial derivatives of the position and velocity with respect to the EqOE, and the inverse of that matrix, along with the Lagrange and Poisson brackets. The authors discussed the advantages of the EqOE with respect to the universal variables for computing general perturbations of planets. In a subsequent paper, Cefola (1972) focused instead on their use as a special perturbation method and obtained single-averaged variational equations in Lagrange's form for different perturbing forces, showing also some numerical results. Moreover, an alternative set of EqOE was presented that is non-singular for $i = \pi$ (the singularity is moved to $i = 0$).

Thanks to the renewed interest in the EqOE showed in the early 1970s, they became very appealing for orbit computation programs. For example, the theory of motion of artificial satellites around the Earth known as Draper Semianalytic Satellite Theory (see Danielson et al. 1995, and references therein) is based on these elements. Furthermore, Junkins et al. (1996) showed that the orbital elements can be more effective than the Cartesian coordinates in predicting the shape of uncertainty distributions with the linear error theory, especially when the observed arc is sufficiently wide. However, classical orbital elements are strongly affected by nonlinearities arising from small values of inclination and eccentricity, while non-singular elements, such as the EqOE, are well-suited for the representation of uncertainties also in these situations (Milani and Gronchi 2010, pp. 120–121). An important advance in this research field is due to Horwood et al. (2011), who replaced the semi-major axis with the mean motion. The resulting *alternate* set of elements (AEqOE) preserves Gaussianity of the initial state uncertainty through its propagation at any time in a pure two-body dynamics. This property was already noticed by Milani and Gronchi (2010, Sect. 7.4) for the *orbit identification* problem. Curiously enough, the mean motion appears as one of the elements in the aforementioned paper by Arsenault et al. (1970).

Generalizations of the EqOE that account for perturbing forces in the elements definition have been proposed. In a recent work, Aristoff et al. (2021) show the improvement in nonlinear uncertainty propagation obtained by a set of "J_2 equinoctial orbital elements (J_2EqOE)". The proposed elements are defined through a multistep iterative algorithm that hinges on the Brouwer–Lyddane solution of the J_2-perturbed satellite problem. No direct ordinary differential equations are provided for the evolution of these elements. Another relatively recent contribution is due to Biria and Russell (2018), who introduced the *oblate spheroidal* equinoctial orbital elements, which are formally defined as the *modified* EqOE of Walker et al. (1985), using spheroidal elements based on Vinti's (1959) theory in place of Keplerian elements. The new equinoctial elements have been used by Biria and Russell (2020) to write the analytical solution of Vinti's problem.

In this paper, we propose a generalization of the EqOE, which is possible when some or all of the perturbing forces are derivable from a potential energy $\mathscr{U}$. They have been designed especially for improving orbit computation of Earth's satellites. In Sect. 2, we describe how

$\mathscr{U}$ can be embedded in the definitions of the generalized semi-major axis (a) and generalized Laplace vector ($\mu\mathbf{g}$), which fix a non-osculating ellipse on the orbital plane at every instant of time. The projections of $\mathbf{g}$ along the in-plane axes of the equinoctial reference frame define p_1, p_2, i.e., the generalized versions of the elements h, k. Kepler's equation is written in a new form where the generalized mean longitude $\mathcal{L}$ or $\mathcal{L}_0$ appears. The generalized mean motion ν and the quantities q_1, q_2, which coincide with p, q in (1), complete our set of *generalized equinoctial orbital elements*, hereafter GEqOE. The idea behind the proposed method is the same that led to the development of two non-singular sets of orbital elements known as DromoP and EDromo (Baù et al. 2013, 2015). We remark that while DromoP and EDromo employ redundant variables, the GEqOE consist of six quantities only: ν, p_1, p_2, $\mathcal{L}$ (or $\mathcal{L}_0$), q_1, q_2.

In Sects. 3–6, we report the transformation from position and velocity to the GEqOE and its inverse, the time derivatives of the GEqOE, and the Jacobian matrix of the transformation together with the inverse of this matrix. In Sect. 7, we include some numerical tests to evaluate the orbit propagation performance of our new elements against the alternate EqOE as well as the Cartesian elements (i.e., Cowell's method). Conclusions and future developments of this work are contained in Sect. 8. Finally, in Appendix B we show through an explicit computation the step-by-step procedure to convert to and from GEqOE and Cartesian position and velocity coordinates.

2 Derivation of the new elements

Consider a point P of mass m, which represents a small body (e.g., a spacecraft), subject to the gravitational attraction of a body of mass M (e.g., a planet). We introduce a reference frame

$$\Sigma = \{O; \mathbf{e}_x, \mathbf{e}_y, \mathbf{e}_z\}, \tag{2}$$

with its origin in the center of mass O of the planet and unit vectors fixed in space. Let $\mathbf{r}$ be the position of P relative to O, and $\dot{\mathbf{r}}$ the time derivative of $\mathbf{r}$ in Σ. The point mass is also subject to the perturbing force $\mathbf{F}$, which is assumed to be the sum of two contributions:

$$\mathbf{F}(\mathbf{r}, \dot{\mathbf{r}}, t) = \mathbf{P}(\mathbf{r}, \dot{\mathbf{r}}, t) - \nabla\mathscr{U}(\mathbf{r}, t). \tag{3}$$

The vector $\mathbf{P}$ represents the perturbing force that does not arise from a potential, while $-\nabla\mathscr{U}$ denotes the perturbing force that arises from the potential energy $\mathscr{U}$, which depends on $\mathbf{r}$ and possibly on time t. For future use, we introduce the *orbital* reference frame $\Sigma_{\text{or}} = \{O; \mathbf{e}_r, \mathbf{e}_f, \mathbf{e}_h\}$, where

$$\mathbf{e}_r = \frac{\mathbf{r}}{|\mathbf{r}|}, \quad \mathbf{e}_f = \mathbf{e}_h \times \mathbf{e}_r, \quad \mathbf{e}_h = \frac{\mathbf{r} \times \dot{\mathbf{r}}}{|\mathbf{r} \times \dot{\mathbf{r}}|}. \tag{4}$$

In the remainder of the paper, we will refer to the *equinoctial orbital elements* to indicate the set of elements presented in Broucke and Cefola (1972).

2.1 The non-osculating ellipse Γ

Let $h = |\mathbf{r} \times \dot{\mathbf{r}}|$ be the magnitude of the angular momentum vector of P with respect to O and $r = |\mathbf{r}|$ the orbital distance. Assume that r and h are strictly positive quantities. We define

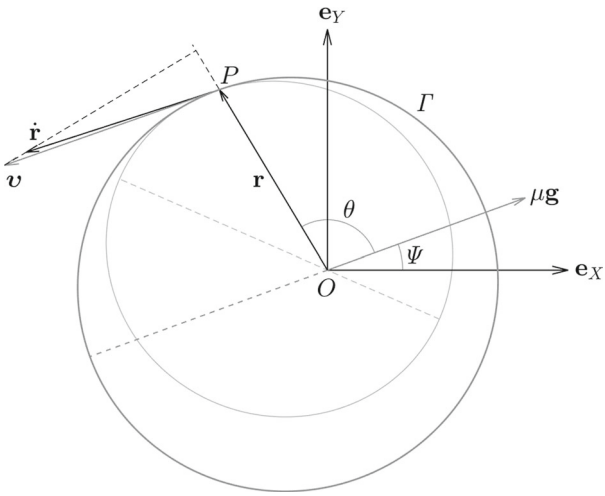

Fig. 1 View from the angular momentum vector of the *osculating* ellipse (in light gray) and the *non-osculating* ellipse Γ described in Sect. (2.1). The generalized true anomaly θ and generalized longitude of pericenter Ψ are also shown. The velocities $\dot{\mathbf{r}}$ and $\boldsymbol{\upsilon}$ of P along the two ellipses have the same radial component $\dot{r}$

the *effective* potential energy as

$$\mathscr{U}_{\text{eff}} = \frac{h^2}{2r^2} + \mathscr{U}. \tag{5}$$

Then, the total energy $\mathscr{E}$ can be written in the form

$$\mathscr{E} = \frac{1}{2}\dot{r}^2 - \frac{\mu}{r} + \mathscr{U}_{\text{eff}},$$

where $\dot{r}$ is the radial velocity and $\mu = G(M + m)$, with G the gravitational constant. We introduce the generalized angular momentum

$$c = \sqrt{2r^2\mathscr{U}_{\text{eff}}}, \tag{6}$$

and the generalized velocity vector

$$\boldsymbol{\upsilon} = \dot{r}\,\mathbf{e}_r + \frac{c}{r}\mathbf{e}_f. \tag{7}$$

From now on, let us assume that $\mathscr{E} < 0$. The pair of vectors $(\mathbf{r}, \boldsymbol{\upsilon})$ defines a *non-osculating* ellipse Γ, having one focus located at the center of mass of the primary body of attraction. Its shape is fixed by the generalized semi-major axis and generalized eccentricity, given by

$$a = -\frac{\mu}{2\mathscr{E}}, \tag{8}$$

$$g = \frac{1}{\mu}\sqrt{\mu^2 + 2\mathscr{E}c^2}. \tag{9}$$

Denoting by e the eccentricity and by $\mathscr{E}_K$ the Keplerian energy, we find

$$g^2 = e^2 + \frac{2\mathscr{U}}{\mu^2}\left[h^2 + 2r^2(\mathscr{E}_K + \mathscr{U})\right].$$

The ellipse Γ lies on the orbital plane, and its orientation on this plane is fixed by the generalized Laplace vector (see Fig. 1)

$$\mu\mathbf{g} = \boldsymbol{\upsilon} \times (\mathbf{r} \times \boldsymbol{\upsilon}) - \mu\mathbf{e}_r, \tag{10}$$

where $|\mathbf{g}| = g$.

Remark 1 Note that when $\dot{r} = 0$, P is at the pericenter/apocenter of both the osculating conic defined by the Keplerian orbital elements and the non-osculating ellipse Γ.

Let us introduce the generalized true anomaly θ through the relations

$$g\cos\theta = \frac{c^2}{\mu r} - 1, \tag{11}$$

$$g\sin\theta = \frac{c\dot{r}}{\mu}, \tag{12}$$

which are analogous to the well-known relations for the Kepler problem

$$e\cos f = \frac{h^2}{\mu r} - 1,$$

$$e\sin f = \frac{h\dot{r}}{\mu},$$

where f is the true anomaly. The angle θ allows us to recover the orientation of the radial direction from that of $\mathbf{g}$.

2.2 The elements $\nu, p_1, p_2, \mathcal{L}$

Consider the classical equinoctial reference frame

$$\Sigma_{\text{eq}} = \{O; \mathbf{e}_X, \mathbf{e}_Y, \mathbf{e}_Z\}.$$

The corresponding coordinate axes are defined with respect to Σ (see equation 2) as follows (Battin 1999, p. 494): a clockwise rotation about $\mathbf{e}_z$ of the longitude Ω fixes the direction of the ascending node[1], a clockwise rotation around this axis of the orbital inclination i establishes the direction of $\mathbf{e}_Z$, and a counterclockwise rotation of Ω around the direction of $\mathbf{e}_Z$ gives the axis associated with $\mathbf{e}_X$. The angular displacement between the direction of $\mathbf{e}_r$ and the *departure* direction defined by $\mathbf{e}_X$ is called true longitude and is given by

$$L = \varpi + f, \tag{13}$$

where

$$\varpi = \omega + \Omega,$$

with ω the argument of pericenter. For later use, we write the projections of the angular velocity of Σ_{eq} with respect to Σ onto the equinoctial axes as[2]

$$\begin{aligned} w_X &= F_h \frac{r}{h}\cos L, \\ w_Y &= F_h \frac{r}{h}\sin L, \\ w_h &= -\frac{r}{h} F_h \tan\frac{i}{2}\sin(\omega + f), \end{aligned} \tag{14}$$

where $F_h = \mathbf{F}\cdot\mathbf{e}_h$. Note that w_h is not defined if $i = \pi$.

[1] If the line of nodes is not defined we can set $\Omega = 0$.

[2] The expression of w_h is obtained using (67).

Let us introduce the angular variable Ψ:

$$\Psi = L - \theta. \tag{15}$$

When $\mathscr{U} = 0$, the angle θ coincides with f and thereby $\Psi = \varpi$, which becomes constant if $\mathbf{P} = \mathbf{0}$. It is straightforward to check that through the angle Ψ we can obtain the direction of the Laplace vector from the direction of $\mathbf{e}_X$, and for this reason we call it the generalized longitude of pericenter (see Fig. 1).

The first three elements of the new set are defined as

$$\nu := \frac{1}{\mu}(-2\mathscr{E})^{3/2}, \tag{16}$$

$$p_1 := g \sin \Psi, \tag{17}$$

$$p_2 := g \cos \Psi, \tag{18}$$

where ν is the generalized form of the mean motion n, and p_1, p_2 are the generalized versions of the equinoctial orbital elements h, k (Broucke and Cefola 1972). For later use, we introduce the generalized semi-latus rectum

$$\varrho = a(1 - g^2), \tag{19}$$

and note that the following formula holds:

$$c^2 = \mu\varrho, \tag{20}$$

which is obtained from (8), (9), (19). Moreover, since

$$a = \left(\frac{\mu}{\nu^2}\right)^{1/3}, \tag{21}$$

$$g^2 = p_1^2 + p_2^2, \tag{22}$$

we can write c as a function of ν, p_1, and p_2:

$$c = \left(\frac{\mu^2}{\nu}\right)^{1/3} \sqrt{1 - p_1^2 - p_2^2}. \tag{23}$$

At this point, we need to make another step to define the fourth generalized equinoctial element. We first introduce the generalized eccentric anomaly G through the relations

$$r = a(1 - g \cos G), \tag{24}$$

$$r\dot{r} = g\sqrt{\mu a} \sin G, \tag{25}$$

which are analogous to the well-known relations for the Kepler problem

$$r = a(1 - e \cos E),$$
$$r\dot{r} = e\sqrt{\mu a} \sin E,$$

where a and E are the semi-major axis and eccentric anomaly, respectively. Then, the generalized Kepler's equation can be written as

$$\mathcal{M} = G - g \sin G, \tag{26}$$

where $\mathcal{M}$ is the generalized mean anomaly

$$\mathcal{M} = \nu(t - t_0), \tag{27}$$

and t_0 is the time of passage through the pericenter of the ellipse Γ (see Remark 1).

We include in the GEqOE the generalized mean longitude

$$\mathcal{L} := \mathcal{M} + \Psi. \tag{28}$$

After defining in a similar way the generalized eccentric longitude as

$$\mathcal{K} = G + \Psi, \tag{29}$$

we can put equation (26) in the form

$$\mathcal{L} = \mathcal{K} + p_1 \cos\mathcal{K} - p_2 \sin\mathcal{K}, \tag{30}$$

where the right-hand side is derived by taking into account (17), (18), (28), (29). If we know the values of p_1, p_2, and $\mathcal{L}$, we can compute $\mathcal{K}$ by solving Kepler's equation (30). The orbital distance and the radial velocity are obtained by means of the formulae:

$$r = a(1 - p_1 \sin\mathcal{K} - p_2 \cos\mathcal{K}), \tag{31}$$

$$\dot{r} = \frac{\sqrt{\mu a}}{r}(p_2 \sin\mathcal{K} - p_1 \cos\mathcal{K}), \tag{32}$$

which follow from eqs (24), (25) where we use definitions (17), (18), (29). Considering also relation (21), we recognize that r and $\dot{r}$ are known from the first four GEqOE, i.e., ν, p_1, p_2, $\mathcal{L}$, which are defined in eqs (16), (17), (18), (28).

It is worth noting that r and $\dot{r}$ can also be expressed as functions of the true longitude. From eqs (11), (12) and (15), (17), (18), we have

$$r = \frac{\varrho}{1 + p_1 \sin L + p_2 \cos L}, \tag{33}$$

$$\dot{r} = \frac{\mu}{c}(p_2 \sin L - p_1 \cos L), \tag{34}$$

where ϱ is introduced in (19).

2.3 The remaining elements

The three elements ν, p_1, p_2 determine the shape and orientation of the non-osculating ellipse Γ on the orbital plane, and $\mathcal{L}$ fixes the position of P with respect to Σ_{eq}. Therefore, the remaining elements of the proposed set need to characterize the orientation of Σ_{eq} with respect to Σ (see equation 2), which can be recovered by applying the sequence of rotations $\Omega, i, -\Omega$.

The two elements p, q in Broucke and Cefola (1972), that is:

$$q_1 := \tan\frac{i}{2}\sin\Omega, \tag{35}$$

$$q_2 := \tan\frac{i}{2}\cos\Omega \tag{36}$$

satisfy our request, and therefore, it is natural to include them in the set of GEqOE. Another possible choice is represented by the Euler parameters e_1, e_2, e_3, e_4 (Goldstein 1980, p. 155) that define the orientation of Σ_{eq} with respect to Σ. We refer to Appendix A for more details about this alternative formulation.

2.4 Summary

A set of *generalized equinoctial orbital elements* consists of

$$\nu \text{ (eq. 16)}, \quad p_1 \text{ (eq. 17)}, \quad p_2 \text{ (eq. 18)}, \quad \mathcal{L} \text{ (eq. 28)},$$

along with

$$q_1 \text{ (eq. 35)}, \quad q_2 \text{ (eq. 36)}.$$

The generalized mean longitude $\mathcal{L}$ can be replaced by the generalized mean longitude at epoch $\mathcal{L}_0$ as shown in Sect. 5.1. These sets of elements represent two generalizations of the alternate equinoctial orbital elements proposed by Horwood et al. (2011) (see the Introduction), with an improved propagation performance, as it will be shown in Sect. 7.

Remark 2 If $\mathscr{E} > 0$, the proposed generalization is not defined. However, restrictions on the values of the total energy can be avoided if the quantities ν and $\mathcal{L}$ are replaced by the generalized semi-latus rectum ϱ (19) and the true longitude L (13), respectively. A consequent benefit coming from employing the elements ϱ, p_1, p_2, L, q_1, q_2, is that we do not need to solve Kepler's equation. This set may result particularly suitable for orbit transfer problems (see Kéchichian 2018, Ch. 9).

3 From position and velocity to the new elements

Assume that we know the position ($\mathbf{r}$) and velocity ($\dot{\mathbf{r}}$) at some time t with respect to the reference frame Σ. We want to determine the values of the new elements.

First, we get the unit vectors $\mathbf{e}_r, \mathbf{e}_f, \mathbf{e}_h$ of the orbital reference frame using their definition in (4), and the quantities

$$r = |\mathbf{r}|, \qquad \dot{r} = \frac{\mathbf{r}\cdot\dot{\mathbf{r}}}{r}, \qquad h = |\mathbf{r}\times\dot{\mathbf{r}}|.$$

We compute the total energy

$$\mathscr{E}(\mathbf{r},\dot{\mathbf{r}},t) = \mathscr{E}_K(\mathbf{r},\dot{\mathbf{r}}) + \mathscr{U}(\mathbf{r},t),$$

where $\mathscr{E}_K$ is the Keplerian energy and the function $\mathscr{U}$ does not depend on $\dot{\mathbf{r}}$. The element ν is obtained from eq (16).

The elements q_1, q_2 are given by (see Cefola 1972, where q_1, q_2 are denoted by p, q, respectively):

$$q_1 = \frac{\mathbf{e}_h\cdot\mathbf{e}_x}{1+\mathbf{e}_h\cdot\mathbf{e}_z}, \qquad q_2 = \frac{-\mathbf{e}_h\cdot\mathbf{e}_y}{1+\mathbf{e}_h\cdot\mathbf{e}_z}.$$

For the unit vectors $\mathbf{e}_X, \mathbf{e}_Y, \mathbf{e}_Z$ of the equinoctial reference frame we apply the formulae

$$\begin{aligned}
\mathbf{e}_X &= \frac{1}{1+q_1^2+q_2^2}\left(1-q_1^2+q_2^2,\ 2q_1q_2,\ -2q_1\right)^T,\\
\mathbf{e}_Y &= \frac{1}{1+q_1^2+q_2^2}\left(2q_1q_2,\ 1+q_1^2-q_2^2,\ 2q_2\right)^T,\\
\mathbf{e}_Z &= \frac{1}{1+q_1^2+q_2^2}\left(2q_1,\ -2q_2,\ 1-q_1^2-q_2^2\right)^T.
\end{aligned} \tag{37}$$

After computing in sequence c, $\boldsymbol{\upsilon}$, and $\mathbf{g}$ from eqs (6), (7), and (10), we can find the values of the elements p_1, p_2 from the two projections

$$p_1 = \mathbf{g} \cdot \mathbf{e}_Y, \qquad p_2 = \mathbf{g} \cdot \mathbf{e}_X.$$

Finally, we want to determine the generalized mean longitude $\mathcal{L}$. We first find the position coordinates in Σ_{eq}:

$$X = \mathbf{r} \cdot \mathbf{e}_X, \qquad Y = \mathbf{r} \cdot \mathbf{e}_Y.$$

Then, we obtain $\mathcal{L}$ from the generalized Kepler's equation (30) written as

$$\mathcal{L} = \operatorname{atan2}(\sin \mathcal{K}, \cos \mathcal{K}) + \frac{1}{a\beta}(Xp_1 - Yp_2), \tag{38}$$

where a is a function of ν and the constant μ, only (see 21),

$$\begin{aligned} \cos \mathcal{K} &= p_2 + \frac{1}{a\beta}[(1 - \alpha p_2^2)X - \alpha p_1 p_2 Y], \\ \sin \mathcal{K} &= p_1 + \frac{1}{a\beta}[(1 - \alpha p_1^2)Y - \alpha p_1 p_2 X], \end{aligned} \tag{39}$$

and

$$\alpha = \frac{1}{1+\beta}, \qquad \beta = \sqrt{1 - p_1^2 - p_2^2}. \tag{40}$$

In Appendix D, we explain how eqs (38) and (39) can be obtained.

4 From the new elements to position and velocity

Assume now that we know the values taken by the new elements at some time t and we want to find $\mathbf{r}$ and $\dot{\mathbf{r}}$ at that epoch.

We first solve Kepler's equation (30) for $\mathcal{K}$. Then, we get the unit vectors $\mathbf{e}_X$, $\mathbf{e}_Y$ of the equinoctial reference frame from (37). The position and velocity vectors can be expressed as

$$\begin{aligned} \mathbf{r} &= X\mathbf{e}_X + Y\mathbf{e}_Y, \\ \dot{\mathbf{r}} &= \dot{X}\mathbf{e}_X + \dot{Y}\mathbf{e}_Y. \end{aligned} \tag{41}$$

We compute the coordinates X, Y through the formulae (see Appendix D)

$$\begin{aligned} X &= a\left[\alpha p_1 p_2 \sin \mathcal{K} + (1 - \alpha p_1^2)\cos \mathcal{K} - p_2\right], \\ Y &= a\left[\alpha p_1 p_2 \cos \mathcal{K} + (1 - \alpha p_2^2)\sin \mathcal{K} - p_1\right], \end{aligned} \tag{42}$$

where a, α are obtained from (21), (40).

For the coordinates $\dot{X}$, $\dot{Y}$, we have

$$\begin{aligned} \dot{X} &= \dot{r}\cos L - \frac{h}{r}\sin L, \\ \dot{Y} &= \dot{r}\sin L + \frac{h}{r}\cos L, \end{aligned} \tag{43}$$

where r, $\dot{r}$ are obtained from (31), (32), and

$$\cos L = \frac{X}{r}, \qquad \sin L = \frac{Y}{r}.$$

Finally, noting that the function $\mathscr{U}$ does not depend on $\dot{\mathbf{r}}$, we can use eq (6) to calculate h:

$$h = \sqrt{c^2 - 2r^2\mathscr{U}(\mathbf{r}, t)}, \tag{44}$$

where c^2 is given by (23).

Remark 3 The procedure outlined in this section and in the previous one follows closely Cefola (1972). The only difference is that analogous eqs to (29) and (30) of that paper cannot be written here for $\dot{X}, \dot{Y}$. □

5 Time derivatives of the new elements

We write the time derivatives of the new elements using the orbital basis defined in (4). As shown in Kéchichian (2018, Ch. 8) for the classical equinoctial elements, this basis allows us to obtain compact expressions.
The time derivative of ν is given by

$$\dot{\nu} = -3\left(\frac{\nu}{\mu^2}\right)^{1/3}\dot{\mathscr{E}}, \tag{45}$$

where

$$\dot{\mathscr{E}} = \mathscr{U}_t + \dot{r}P_r + \frac{h}{r}P_f. \tag{46}$$

In the preceding expression, we have $P_r = \mathbf{P}\cdot\mathbf{e}_r$, $P_f = \mathbf{P}\cdot\mathbf{e}_f$, and $\mathscr{U}_t$ is the partial derivative of $\mathscr{U}(\mathbf{r}, t)$ with respect to t.

For the time derivatives of p_1, p_2, we have (see the derivation in Appendix E)

$$\begin{aligned}\dot{p}_1 &= p_2\left(\frac{h-c}{r^2} - w_h\right) + \frac{1}{c}\left(\frac{X}{a} + 2p_2\right)(2\mathscr{U} - rF_r)\\ &\quad + \frac{1}{c^2}\left[Y(r+\varrho) + r^2p_1\right]\dot{\mathscr{E}}, \end{aligned}\tag{47}$$

$$\begin{aligned}\dot{p}_2 &= p_1\left(w_h - \frac{h-c}{r^2}\right) - \frac{1}{c}\left(\frac{Y}{a} + 2p_1\right)(2\mathscr{U} - rF_r)\\ &\quad + \frac{1}{c^2}\left[X(r+\varrho) + r^2p_2\right]\dot{\mathscr{E}}, \end{aligned}\tag{48}$$

where $F_r = \mathbf{F}\cdot\mathbf{e}_r$ and $\varrho = c^2/\mu$.
Concerning the element $\mathcal{L}$, we can write (see the derivation in Appendix F)

$$\dot{\mathcal{L}} = \nu + \frac{h-c}{r^2} - w_h + \frac{1}{c}\left[\frac{1}{\alpha} + \alpha\left(1 - \frac{r}{a}\right)\right](2\mathscr{U} - rF_r) + \frac{r\dot{r}\alpha}{\mu c}(r+\varrho)\dot{\mathscr{E}}, \tag{49}$$

where α is defined in (40). Finally, the time derivatives of q_1, q_2 read (see Battin 1999, eqs. 10.51, 10.52, p. 493)

$$\dot{q}_1 = \frac{1}{2}w_Y(1 + q_1^2 + q_2^2), \tag{50}$$

$$\dot{q}_2 = \frac{1}{2}w_X(1 + q_1^2 + q_2^2). \tag{51}$$

We observe that the out-of-plane component of $\mathbf{F}$ appears through the quantities w_X, w_Y, w_h previously introduced in (14), which can be computed from

$$w_X = \frac{X}{h} F_h, \qquad w_Y = \frac{Y}{h} F_h, \qquad w_h = w_X q_1 - w_Y q_2. \tag{52}$$

Numerical integration of (45), (47)–(51) allows us to obtain the time evolution of the new elements. For an efficient evaluation of the right-hand side of these differential equations, we can follow the procedure described in Sect. 4. Moreover, we suggest to apply in (49) and (53) the substitutions

$$1 - \frac{r}{a} = p_1 \sin \mathcal{K} + p_2 \cos \mathcal{K}, \qquad \frac{r\dot{r}}{c} = \frac{1}{\beta}(p_2 \sin \mathcal{K} - p_1 \cos \mathcal{K}).$$

Finally, the unit vectors $\mathbf{e}_r$, $\mathbf{e}_f$, $\mathbf{e}_h$, which may be used to find the projections F_r, F_h, P_r, P_f, are obtained as

$$\mathbf{e}_r = \mathbf{e}_X \cos L + \mathbf{e}_Y \sin L, \qquad \mathbf{e}_f = \mathbf{e}_Y \cos L - \mathbf{e}_X \sin L, \qquad \mathbf{e}_h = \mathbf{e}_Z,$$

where $\mathbf{e}_X$, $\mathbf{e}_Y$, $\mathbf{e}_Z$ are given in (37).

5.1 Constant time element

The equinoctial elements presented in Broucke and Cefola (1972) comprise the mean longitude at epoch $\lambda_0 = \varpi + nt_0$, where we recall that n is the mean motion and t_0 the time of pericenter passage. This quantity is a constant of the motion when the perturbations are turned off, and being related to the physical time we can refer to λ_0 as a *constant* time element. On the other hand, the generalized mean longitude $\mathcal{L}$ included in the GEqOE varies linearly with time along Keplerian motion (see eq 49), and therefore, it is a *linear* time element (Stiefel and Scheifele 1971, Ch. 5).

In place of $\mathcal{L}$, we may consider the generalized mean motion at epoch $\mathcal{L}_0$, which we define as[3]

$$\mathcal{L}_0 := \Psi - \nu t_0.$$

Using eqs (27), (28), we see that

$$\mathcal{L}_0 = \mathcal{L} - \nu t,$$

and therefore its time derivative can be computed from (45), (49), resulting in

$$\begin{aligned} \dot{\mathcal{L}}_0 = \frac{h-c}{r^2} - w_h + \frac{1}{c}\left[\frac{1}{\alpha} + \alpha\left(1 - \frac{r}{a}\right)\right](2\mathscr{U} - r F_r) \\ + \left[3t\left(\frac{\nu}{\mu^2}\right)^{1/3} + \frac{r\dot{r}\alpha}{\mu c}(r + \varrho)\right]\dot{\mathscr{E}}. \end{aligned} \tag{53}$$

We note that a term dependent explicitly on time arises in the expression of $\dot{\mathcal{L}}_0$, which is not present in $\dot{\mathcal{L}}$. For long-term propagations, this term may grow enough to deteriorate the efficiency of the propagation.

[3] Another possible definition is $\tilde{\mathcal{L}}_0 := \Psi + \nu t_0$, which represents a direct generalization of the element λ_0.

6 The fundamental matrix and its inverse

The fundamental matrix is defined as the matrix of the partial derivatives of position and velocity with respect to the set of elements used for describing the motion (Broucke 1970). We consider in this section the two sets of GEqOE given by ν, p_1, p_2, q_1, q_2, along with either $\mathcal{L}$ or $\mathcal{L}_0$. In Broucke and Cefola (1972), the fundamental matrix and its inverse are expressed using the perifocal basis. In Danielson et al. (1995), the equinoctial basis, which avoids the singularity for zero eccentricity, is used instead. Here, we adopt the orbital basis $\{\mathbf{e}_r, \mathbf{e}_f, \mathbf{e}_h\}$, which leads to quite compact and elegant expressions for the partials.

In the following, we will use the auxiliary quantities

$$\gamma = 1 + q_1^2 + q_2^2$$

and

$$\xi = p_2 + \cos L, \qquad \zeta = p_1 + \sin L.$$

6.1 Partial derivatives of position and velocity with respect to the GEqOE

We obtain the partial derivatives of $\mathbf{r}, \dot{\mathbf{r}}$ with respect to the GEqOE by direct differentiation of both sides of eqs (41), wherein X, Y and $\dot{X}$, $\dot{Y}$ are replaced by the expressions given in (61) and (43), respectively. Relations (30), (31), (32), (37), (44), (60) are also used. Regarding the position, we have:

$$\begin{aligned}
\frac{\partial \mathbf{r}}{\partial \nu} &= -\frac{2r}{3\nu}\mathbf{e}_r,\\
\frac{\partial \mathbf{r}}{\partial p_1} &= -\Big(\frac{\alpha\dot{r}}{\nu}p_2 + a\sin L\Big)\mathbf{e}_r - a\bigg[\Big(\frac{a\alpha\beta}{r} + \frac{r}{\varrho}\Big)p_2 + \frac{X}{\varrho} + \cos L\bigg]\mathbf{e}_f,\\
\frac{\partial \mathbf{r}}{\partial p_2} &= \Big(\frac{\alpha\dot{r}}{\nu}p_1 - a\cos L\Big)\mathbf{e}_r + a\bigg[\Big(\frac{a\alpha\beta}{r} + \frac{r}{\varrho}\Big)p_1 + \frac{Y}{\varrho} + \sin L\bigg]\mathbf{e}_f,\\
\frac{\partial \mathbf{r}}{\partial \mathcal{L}} &= \frac{1}{\nu}\boldsymbol{\upsilon},\\
\frac{\partial \mathbf{r}}{\partial q_1} &= -\frac{2}{\gamma}(rq_2\mathbf{e}_f + X\mathbf{e}_h),\\
\frac{\partial \mathbf{r}}{\partial q_2} &= \frac{2}{\gamma}(rq_1\mathbf{e}_f + Y\mathbf{e}_h),
\end{aligned} \tag{54}$$

where the generalized velocity $\boldsymbol{\upsilon}$ is introduced in (7) and the non-dimensional quantities α, β in (40).

Remark 4 The derivatives of $\mathbf{r}$ with respect to a, p_1, p_2, $\tilde{\mathcal{L}}_0$ (see the footnote 3), q_1, q_2 can be written in the same form as the derivatives of $\mathbf{r}$ with respect to a, h, k, λ_0, p, q that are reported in Broucke and Cefola (1972, Table I). We just have to replace in the latter ones the osculating eccentric anomaly (E), eccentricity (e), semi-major axis (a), longitude of pericenter ($\omega + \Omega$) by G, g, a, Ψ, respectively, and the unit vectors $\mathbf{e}_p$, $\mathbf{e}_q$ of the perifocal reference frame[4] by their generalized versions $\mathbf{e}'_p$, $\mathbf{e}'_q$, which are defined as (see also Fig. 2)

$$\mathbf{e}'_p = \mathbf{e}_X \cos\Psi + \mathbf{e}_Y \sin\Psi,$$

[4] These two unit vectors are denoted by $\mathbf{P}$, $\mathbf{Q}$ in Broucke and Cefola (1972).

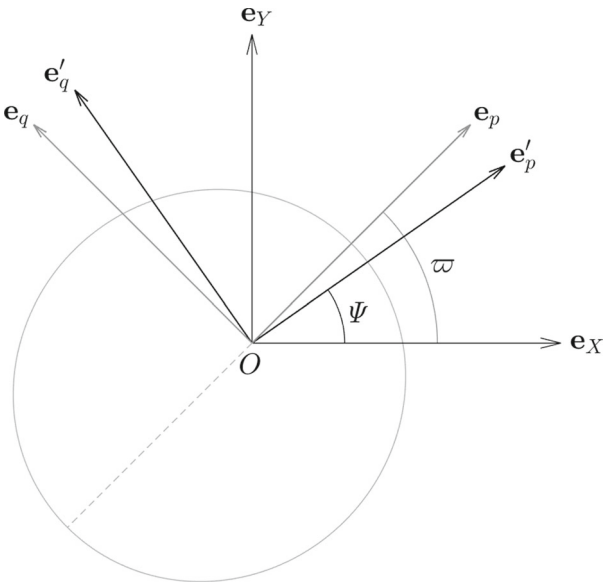

Fig. 2 View from the angular momentum vector of the unit vectors $\mathbf{e}_X, \mathbf{e}_Y$ of the equinoctial basis, and of $\mathbf{e}'_p, \mathbf{e}'_q$, which are the generalized counterparts of the unit vectors $\mathbf{e}_p, \mathbf{e}_q$ of the perifocal basis

$$\mathbf{e}'_q = \mathbf{e}_Y \cos\Psi - \mathbf{e}_X \sin\Psi,$$

where Ψ is given in (15).

The partial derivatives of the velocity with respect to the GEqOE are:

$$\begin{aligned}
\frac{\partial\dot{\mathbf{r}}}{\partial\nu} &= \frac{1}{3\nu}\dot{\mathbf{r}} + \boldsymbol{\delta}_0,\\
\frac{\partial\dot{\mathbf{r}}}{\partial p_1} &= \frac{a}{r}\Big[\frac{\alpha\sqrt{\mu a}}{r}p_2\,\mathbf{e}_r - \Big(\frac{\mu}{h}p_1 + \dot{X}\Big)\mathbf{e}_f\Big] + \frac{a}{\varrho}\xi\,\mathbf{s} + \boldsymbol{\delta}_1,\\
\frac{\partial\dot{\mathbf{r}}}{\partial p_2} &= -\frac{a}{r}\Big[\frac{\alpha\sqrt{\mu a}}{r}p_1\,\mathbf{e}_r + \Big(\frac{\mu}{h}p_2 - \dot{Y}\Big)\mathbf{e}_f\Big] - \frac{a}{\varrho}\zeta\,\mathbf{s} + \boldsymbol{\delta}_2,\\
\frac{\partial\dot{\mathbf{r}}}{\partial\mathcal{L}} &= -\frac{\mu}{r^2\nu}\mathbf{e}_r + \boldsymbol{\delta}_3,\\
\frac{\partial\dot{\mathbf{r}}}{\partial q_1} &= \frac{2}{\gamma}(q_2\mathbf{s} - \dot{X}\mathbf{e}_h) + \boldsymbol{\delta}_4,\\
\frac{\partial\dot{\mathbf{r}}}{\partial q_2} &= -\frac{2}{\gamma}(q_1\mathbf{s} - \dot{Y}\mathbf{e}_h) + \boldsymbol{\delta}_5,
\end{aligned} \tag{55}$$

where

$$\dot{\mathbf{r}} = \dot{r}\mathbf{e}_r + \frac{h}{r}\mathbf{e}_f, \qquad \mathbf{s} = \frac{h}{r}\mathbf{e}_r - \dot{r}\mathbf{e}_f,$$

and the vectors $\boldsymbol{\delta}_i$ $(i = 0, \ldots, 5)$ are equal to zero if $\mathscr{U} = 0$. We have

$$\begin{aligned}
\boldsymbol{\delta}_0 &= \frac{r}{h}\left(\frac{2}{3\nu}\mathscr{U} - \frac{\partial\mathscr{U}}{\partial\nu}\right)\mathbf{e}_f,\\
\boldsymbol{\delta}_1 &= \frac{1}{r^2}(h-c)\,\mathbf{t}_1 + \frac{1}{h}\left[2\Big(\frac{\alpha\dot{r}}{\nu}p_2 + a\sin L\Big)\mathscr{U} - r\frac{\partial\mathscr{U}}{\partial p_1}\right]\mathbf{e}_f,
\end{aligned}$$

$$\boldsymbol{\delta}_2 = \frac{1}{r^2}(c-h)\,\mathbf{t}_2 - \frac{1}{h}\left[2\Big(\frac{\alpha\dot{r}}{\nu}p_1 - a\cos L\Big)\mathscr{U} + r\frac{\partial\mathscr{U}}{\partial p_2}\right]\mathbf{e}_f,$$
$$\boldsymbol{\delta}_3 = \frac{1}{r^2}(c-h)\,\mathbf{t}_3 - \frac{1}{h}\left(\frac{2\dot{r}}{\nu}\mathscr{U} + r\frac{\partial\mathscr{U}}{\partial\mathcal{L}}\right)\mathbf{e}_f,$$
$$\boldsymbol{\delta}_{i+3} = -\frac{r}{h}\frac{\partial\mathscr{U}}{\partial q_i}\mathbf{e}_f, \quad i = 1, 2,$$

with

$$\mathbf{t}_1 = a\Big(\frac{a\alpha\beta}{r}p_2 + \cos L\Big)\mathbf{e}_r + \frac{\alpha\dot{r}}{\nu}p_2\,\mathbf{e}_f,$$
$$\mathbf{t}_2 = a\Big(\frac{a\alpha\beta}{r}p_1 + \sin L\Big)\mathbf{e}_r + \frac{\alpha\dot{r}}{\nu}p_1\,\mathbf{e}_f,$$
$$\mathbf{t}_3 = \frac{1}{\nu}\Big(\frac{c}{r}\mathbf{e}_r + \dot{r}\mathbf{e}_f\Big).$$

If the constant time element $\mathcal{L}_0$ is used instead of $\mathcal{L}$, we have

$$\frac{\partial\mathbf{r}}{\partial\nu} = \frac{1}{\nu}\Big(t\boldsymbol{\upsilon} - \frac{2}{3}\mathbf{r}\Big),$$
$$\frac{\partial\mathbf{r}}{\partial\mathcal{L}_0} = \frac{\partial\mathbf{r}}{\partial\mathcal{L}},$$

and

$$\frac{\partial\dot{\mathbf{r}}}{\partial\nu} = \frac{1}{3\nu}\dot{\mathbf{r}} + \boldsymbol{\delta}_0 + \frac{t}{r^2\nu}\left[\frac{c}{h}(c-h)\,\mathbf{s} - \mu\mathbf{e}_r\right],$$
$$\frac{\partial\dot{\mathbf{r}}}{\partial\mathcal{L}_0} = \frac{\partial\dot{\mathbf{r}}}{\partial\mathcal{L}}.$$

On the other hand, the partial derivatives of $\mathbf{r}$, $\dot{\mathbf{r}}$ with respect to p_1, p_2, q_1, q_2 remain the same as in (54), (55).

Remark 5 The partial derivative of $\mathscr{U}$ with respect to any element χ of our set of GEqOE is computed by the chain rule

$$\frac{\partial\mathscr{U}}{\partial\chi} = \frac{\partial\mathscr{U}}{\partial\mathbf{r}}\frac{\partial\mathbf{r}}{\partial\chi}.$$

6.2 Partial derivatives of the GEqOE with respect to position and velocity

The inverse of the fundamental matrix for the equinoctial elements is obtained in Broucke and Cefola (1972) using the Poisson brackets and the fundamental matrix (see also Broucke 1970). Here, we proceed as follows. As concerns the elements q_1, q_2, we simply write the expressions given in Broucke and Cefola (1972, Table III) for the derivatives of p, q in a suitable form to avoid singularities for small eccentricities and inclinations (as in Danielson et al. 1995, for example). For the generalized mean motion ν, we start from equation (16) and use the definition of the total energy. The computation for the elements p_1, p_2 is done considering relations (33), (34), and taking into account (13). Finally, concerning $\mathcal{L}$ and $\mathcal{L}_0$, equations (30), (31), (32) are used.

The partial derivatives with respect to the position and velocity read[5]

$$
\begin{aligned}
\frac{\partial \nu}{\partial \mathbf{r}} &= -\frac{3a\nu}{r^2}\mathbf{e}_r^T + \tilde{\boldsymbol{\delta}}_0,\\
\frac{\partial p_1}{\partial \mathbf{r}} &= \frac{\zeta}{r}\mathbf{e}_r^T - \frac{h}{cr}\left[\left(2-\frac{c}{h}\right)p_2 + \frac{X}{a}\right]\mathbf{e}_f^T - \frac{p_2\Lambda}{h}\mathbf{e}_h^T + \tilde{\boldsymbol{\delta}}_1,\\
\frac{\partial p_2}{\partial \mathbf{r}} &= \frac{\xi}{r}\mathbf{e}_r^T + \frac{h}{cr}\left[\left(2-\frac{c}{h}\right)p_1 + \frac{Y}{a}\right]\mathbf{e}_f^T + \frac{p_1\Lambda}{h}\mathbf{e}_h^T + \tilde{\boldsymbol{\delta}}_2,\\
\frac{\partial \mathcal{L}}{\partial \mathbf{r}} &= \frac{\dot{r}}{cr}(\varrho\alpha - r\beta)\mathbf{e}_r^T - \frac{h}{cr}\left[2 - \frac{c}{h} + \frac{\alpha}{a}(\varrho - r)\right]\mathbf{e}_f^T - \frac{\Lambda}{h}\mathbf{e}_h^T + \tilde{\boldsymbol{\delta}}_3,\\
\frac{\partial q_1}{\partial \mathbf{r}} &= -\frac{\gamma\dot{Y}}{2h}\mathbf{e}_h^T,\\
\frac{\partial q_2}{\partial \mathbf{r}} &= -\frac{\gamma\dot{X}}{2h}\mathbf{e}_h^T,
\end{aligned}
$$

and

$$
\begin{aligned}
\frac{\partial \nu}{\partial \dot{\mathbf{r}}} &= -\frac{3}{\sqrt{\mu a}}\dot{\mathbf{r}}^T,\\
\frac{\partial p_1}{\partial \dot{\mathbf{r}}} &= -\frac{c}{\mu}\cos L\,\mathbf{e}_r^T + \frac{h}{\mu}\left(2\sin L - \frac{\dot{r}}{c}X\right)\mathbf{e}_f^T + \frac{\lambda p_2}{h}\mathbf{e}_h^T,\\
\frac{\partial p_2}{\partial \dot{\mathbf{r}}} &= \frac{c}{\mu}\sin L\,\mathbf{e}_r^T + \frac{h}{\mu}\left(2\cos L + \frac{\dot{r}}{c}Y\right)\mathbf{e}_f^T - \frac{\lambda p_1}{h}\mathbf{e}_h^T,\\
\frac{\partial \mathcal{L}}{\partial \dot{\mathbf{r}}} &= \left[\frac{c}{\mu r}\alpha(r-\varrho) - \frac{2r}{\sqrt{\mu a}}\right]\mathbf{e}_r^T + \frac{h\dot{r}}{c\mu}\alpha(\varrho + r)\mathbf{e}_f^T + \frac{\lambda}{h}\mathbf{e}_h^T,\\
\frac{\partial q_1}{\partial \dot{\mathbf{r}}} &= \frac{\gamma Y}{2h}\mathbf{e}_h^T,\\
\frac{\partial q_2}{\partial \dot{\mathbf{r}}} &= \frac{\gamma X}{2h}\mathbf{e}_h^T,
\end{aligned}
$$

where

$$
\begin{aligned}
\tilde{\boldsymbol{\delta}}_0 &= -\frac{3}{\sqrt{\mu a}}\frac{\partial \mathscr{U}}{\partial \mathbf{r}},\\
\tilde{\boldsymbol{\delta}}_1 &= \frac{r}{\mu\varrho}(r\zeta + \varrho\sin L)\frac{\partial \mathscr{U}}{\partial \mathbf{r}},\\
\tilde{\boldsymbol{\delta}}_2 &= \frac{r}{\mu\varrho}(r\xi + \varrho\cos L)\frac{\partial \mathscr{U}}{\partial \mathbf{r}},\\
\tilde{\boldsymbol{\delta}}_3 &= \frac{r\dot{r}}{c\mu}(\varrho + r)\alpha\frac{\partial \mathscr{U}}{\partial \mathbf{r}},
\end{aligned}
$$

and

$$
\lambda = Yq_2 - Xq_1, \qquad \Lambda = \dot{Y}q_2 - \dot{X}q_1.
$$

Note that the vectors $\tilde{\boldsymbol{\delta}}_i$ $(i = 0, \ldots, 3)$ are equal to zero if $\mathscr{U} = 0$.

[5] We found a typo in the expression of $\partial\lambda_0/\partial\mathbf{x}$ reported in Broucke and Cefola (1972, Table III): α_5/α_6 has to be replaced by α_5/α_4.

Finally, the partial derivatives of the constant time element $\mathcal{L}_0$ are given by

$$\frac{\partial \mathcal{L}_0}{\partial \mathbf{r}} = \frac{\partial \mathcal{L}}{\partial \mathbf{r}} - 3t\left(\frac{\alpha}{r^2}\mathbf{e}_r^T - \frac{1}{\sqrt{\mu a}}\frac{\partial \mathscr{U}}{\partial \mathbf{r}}\right),$$
$$\frac{\partial \mathcal{L}_0}{\partial \dot{\mathbf{r}}} = \frac{\partial \mathcal{L}}{\partial \dot{\mathbf{r}}} + \frac{3t}{\sqrt{\mu a}}\dot{\mathbf{r}}^T.$$

Remark 6 If $\mathcal{L}_0$ is employed in place of $\mathcal{L}$, terms that are linear in time are introduced in the expressions of $\partial\mathbf{r}/\partial\nu$, $\partial\dot{\mathbf{r}}/\partial\nu$, $\partial\mathcal{L}_0/\partial\mathbf{r}$, $\partial\mathcal{L}_0/\partial\dot{\mathbf{r}}$.

7 Numerical tests

We employ the generalized orbital equinoctial elements (GEqOE) ν, p_1, p_2, $\mathcal{L}$, q_1, q_2 (Sect. 2.4) to propagate the motion of an artificial satellite around the Earth. Starting from the case in which only the perturbation due to the J_2 zonal harmonic of the geopotential is considered, we then add the third-body gravitational attraction of the Moon and the Sun. In all the proposed test cases, the function $-\mathscr{U}$ is given by the J_2 term of the Earth's gravitational potential. We select the four sets of initial conditions in Table 1, which are converted to the GEqOE (their values are given in Appendix B). The new elements are compared to the alternate equinoctial orbital elements (AEqOE) presented in Horwood et al. (2011, Sect. 10.4) and Cowell's method. We deliberately select a very simple numerical integrator, which is a fourth-order Runge–Kutta with a fixed step size, in order to highlight the impact of the particular set of elements on the propagation performance. The errors are computed by taking as *true* the solution obtained by using the Dromo(PC) formulation presented in Baù and Bombardelli (2014) and an adaptive step size Runge–Kutta Dormand-Prince 5(4)7FM method described in Dormand and Prince (1980) with a tolerance of 10^{-13}. Further details about the numerical tests, which may be useful to reproduce our results, are reported in Appendix C.

7.1 The main problem

Let us introduce an Earth-centered inertial reference frame. In particular, we denote by Oz the axis pointing to the North Pole and by $\mathbf{e}_z$ the corresponding unit vector. We consider here the unrealistic case in which the perturbing force $\mathbf{F}$ (see eq 3) is given by

$$\mathbf{F} = -\nabla\mathscr{U}(\mathbf{r}),$$

where $\mathscr{U}$ is the potential energy associated with the J_2 term of the Earth's gravitational field:

$$\mathscr{U} = -\frac{A}{r^3}(1 - 3\hat{z}^2), \tag{56}$$

Table 1 Initial conditions for the numerical tests: r_p is the radius of perigee in km, e, i, Ω, ω, M_0 are Keplerian elements. Angular variables are given in degrees and expressed with respect to the J2000 frame

	r_p	e	i	Ω	ω	M_0
(a)	7178.1366	0	45	0	0	0
(b)	7178.1366	0	0	0	0	0
(c)	7178.1366	0	90	0	0	0
(d)	6916	0.74	63.4	30	270	0

with

$$A = \frac{GMJ_2 r_e^2}{2}, \qquad \hat{z} = \frac{z}{r},$$

and $z = \mathbf{r} \cdot \mathbf{e}_z$. The quantity r_e denotes the equatorial radius of the Earth. We have

$$\mathbf{F} = -\frac{3A}{r^4}\left[(1 - 5\hat{z}^2)\mathbf{e}_r + 2\hat{z}\mathbf{e}_z\right].$$

In the differential equations of the GEqOE, the perturbing force appears in the terms $2\mathscr{U} - rF_r$ and w_h. A straightforward computation yields

$$2\mathscr{U} - rF_r = -\mathscr{U}, \qquad F_h = -\frac{6A}{r^4}\hat{z}\cos i.$$

Moreover, noting that

$$\hat{z} = \frac{2(Yq_2 - Xq_1)}{r(1 + q_1^2 + q_2^2)}, \tag{57}$$

we obtain

$$w_h = I\hat{z},$$

with

$$I = \frac{3A}{hr^3}\hat{z}(1 - q_1^2 - q_2^2). \tag{58}$$

Taking into account that the total energy $\mathscr{E}$ is a first integral in this case, the time derivatives of the GEqOE become

$$\begin{aligned}
\dot{\nu} &= 0,\\
\dot{p}_1 &= p_2\left(\frac{h-c}{r^2} - I\hat{z}\right) - \frac{1}{c}\left(\frac{X}{a} + 2p_2\right)\mathscr{U},\\
\dot{p}_2 &= p_1\left(I\hat{z} - \frac{h-c}{r^2}\right) + \frac{1}{c}\left(\frac{Y}{a} + 2p_1\right)\mathscr{U},\\
\dot{\mathcal{L}} &= \nu + \frac{h-c}{r^2} - I\hat{z} - \frac{1}{c}\left[\frac{1}{\alpha} + \alpha\left(1 - \frac{r}{a}\right)\right]\mathscr{U},\\
\dot{q}_1 &= -I\frac{Y}{r},\\
\dot{q}_2 &= -I\frac{X}{r},
\end{aligned}$$

where $\hat{z}$, I are determined by (57), (58). In the equations above, the quantities a, ν remain constant along the motion and their values are determined from the initial position ($\mathbf{r}$) and velocity ($\dot{\mathbf{r}}$). In particular, the value of the element ν is computed by (see eq 16)

$$\nu = \frac{1}{\mu}\left[\frac{2\mu}{r_*} + \frac{2A}{r_*^3}(1 - 3\hat{z}_*^2) - |\dot{\mathbf{r}}_*|^2\right]^{3/2},$$

where r_*, $\hat{z}_*$, $\dot{\mathbf{r}}_*$ refer to the starting epoch of the propagation.

The initial conditions specified in the row labeled (a) in Table 1, which correspond to a low Earth orbit, are propagated for 12 days. Figure 3 shows the position error at the final time obtained with different values of the integration step size. The same initial conditions are then propagated for 365 days using a step size of 1 minute. The time evolution of the

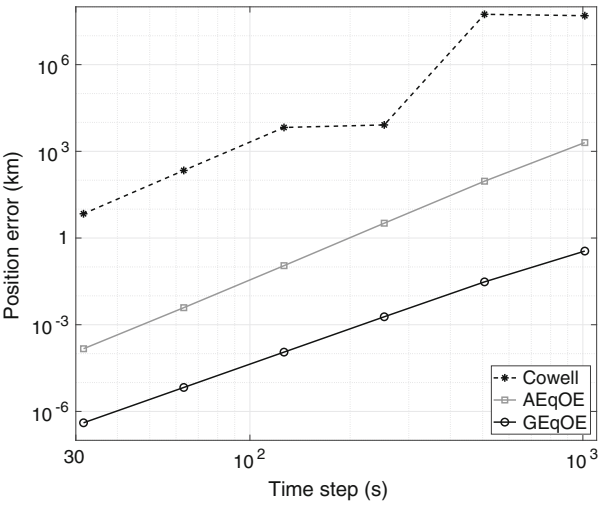

Fig. 3 Position error after 12 days of propagation for increasing values of the integration step size. The initial conditions correspond to the low Earth orbit reported in the row (**a**) of Table 1. Only the perturbation arising from the J_2 zonal harmonic of the geopotential is considered. Note that a logarithmic scale is applied to both axes. The *true* position and velocity at the final epoch are reported in Appendix C

errors in the position and total energy are displayed in Fig. 4. It is evident that the GEqOE are much better than the AEqOE and Cowell's method for this test case.

7.2 J_2 and third-body perturbations

Third-body perturbing forces due to the gravitational attraction of the Moon and the Sun are switched on in the following tests. Note that although third-body perturbations do derive from a potential, we could not observe, at least for the propagation of Earth-bound orbits, any improvement in propagation performance as a result of including that potential in the total energy. As a matter of fact, numerical instability can occur in some cases, especially when ephemeris data are employed. Therefore, we directly considered these forces for the computation of the vector $\mathbf{P}$ in eq (3). On the other hand, the force exerted by the Earth's oblateness is derived from the potential energy $\mathscr{U}$ introduced in (56).

The same performance plots shown in Sect. 7.1 are obtained for the initial conditions reported in the rows (b), (c), and (d) of Table 1, which correspond to a low Earth equatorial orbit, a low Earth polar orbit, and a Molniya orbit, respectively. The initial epoch of the propagations is January 1, 2020 UTC. For a short-term propagation (on the order of a few days), we display in Fig. 5 the variation of the position error referred to the final time as the step size of the integrator is enlarged. Then, for a long-term propagation (on the order of hundreds of days), Fig. 6 shows the time evolution of the position error using a step size of 1 minute. The time span of the Molniya orbit propagation was chosen about 7 times larger in order to have the same number of revolutions as in the case of the two low Earth orbits.

From these results, we see that third-body perturbations do not deteriorate the performance of the GEqOE, when compared to the case in which only a conservative perturbation is present. Therefore, the generalized equinoctial orbital elements bring a substantial improvement with respect to the AEqOE and Cowell's method.

Because the Molniya orbit is quite eccentric, it is reasonable to use also a variable step size numerical integrator: we chose the same Runge–Kutta Dormand–Prince method that provides the *true* solution. The relative tolerance controls the selection of the step size and tighter tolerances imply shorter steps. The total number of evaluations of the vector field

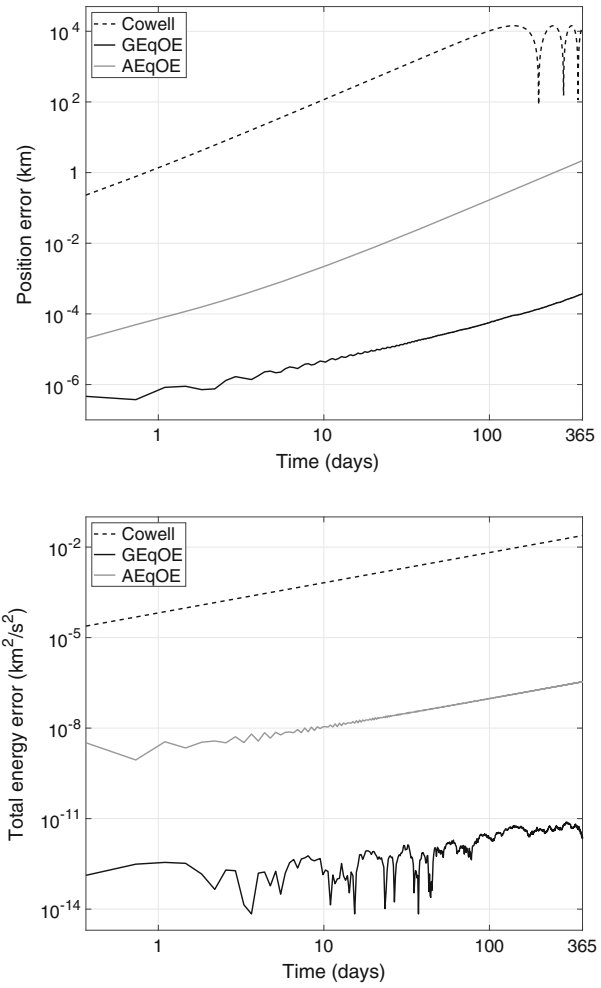

Fig. 4 Time evolution of (*top*) the position error and (*bottom*) the error of the total energy throughout 365 days of propagation of the initial conditions reported in the row (**a**) of Table 1. Only the perturbation arising from the J_2 zonal harmonic of the geopotential is considered. Note that a logarithmic scale is applied to both axes

at the end of the propagation can be taken as a measure of the computational cost. In Fig. 7, we show for decreasing values of the relative tolerance the number of evaluations and the corresponding maximum position error reached in a propagation time of 85.6 days. We denote with GEqOE(c) the set of generalized orbital elements in which $\mathcal{L}_0$ (see Sect. 5.1) is employed instead of $\mathcal{L}$. While in the previous numerical tests GEqOE and GEqOE(c) exhibit an almost identical performance, in this test the latter formulation is better: it is faster and decreases the minimum achievable position error. We see that the formulations GEqOE and GEqOE(c) are much more efficient than the AEqOE and Cowell's method.

8 Conclusions and future work

We have introduced six orbital elements that generalize the classical equinoctial elements in the presence of perturbations that are derivable from a potential. The latter appears in the intrinsic definition of the new elements, through the generalization of different orbital

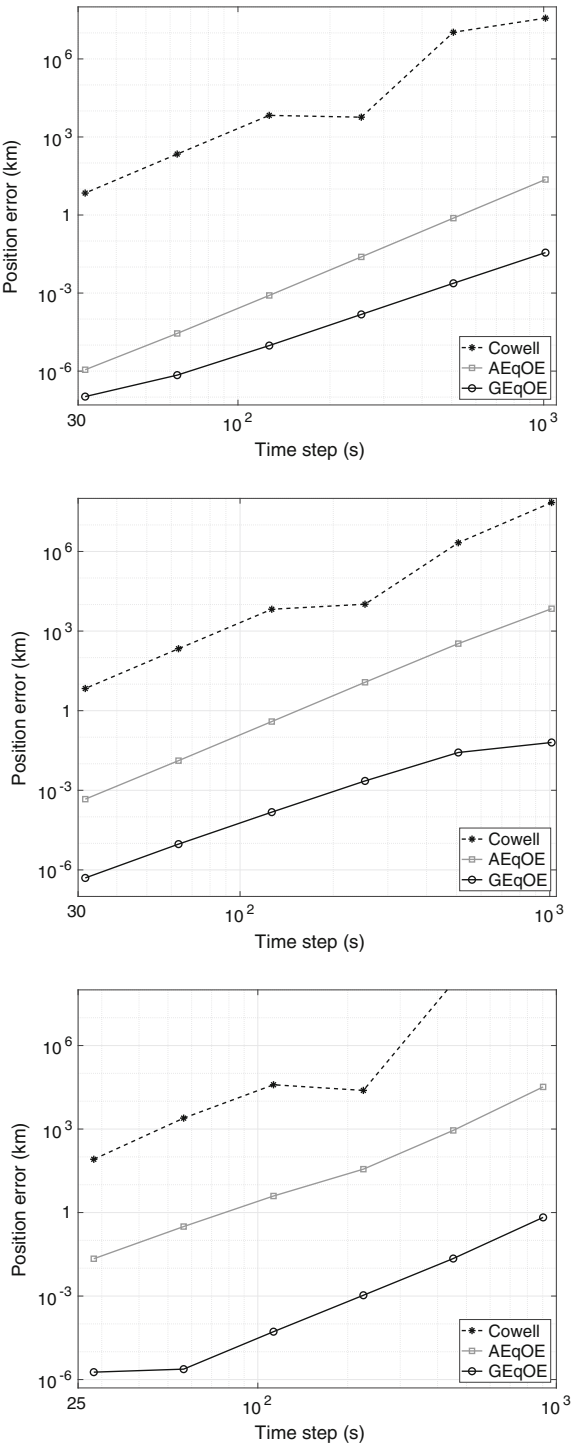

Fig. 5 Position error for increasing values of the integration step size. The initial conditions are reported in the rows (b), (c), and (d) of Table 1 and correspond to (*top*) a low Earth equatorial orbit, (*middle*) a low Earth polar orbit, and (*bottom*) a Molniya orbit, respectively. The first two orbits are propagated for 12 days, the latter for 85.6 days. Perturbations due to the J_2 zonal harmonic of the geopotential and the attraction of the Moon and the Sun are considered. Note that a logarithmic scale is applied to both axes. The *true* position and velocity at the final epoch for each of the three cases are reported in Appendix C

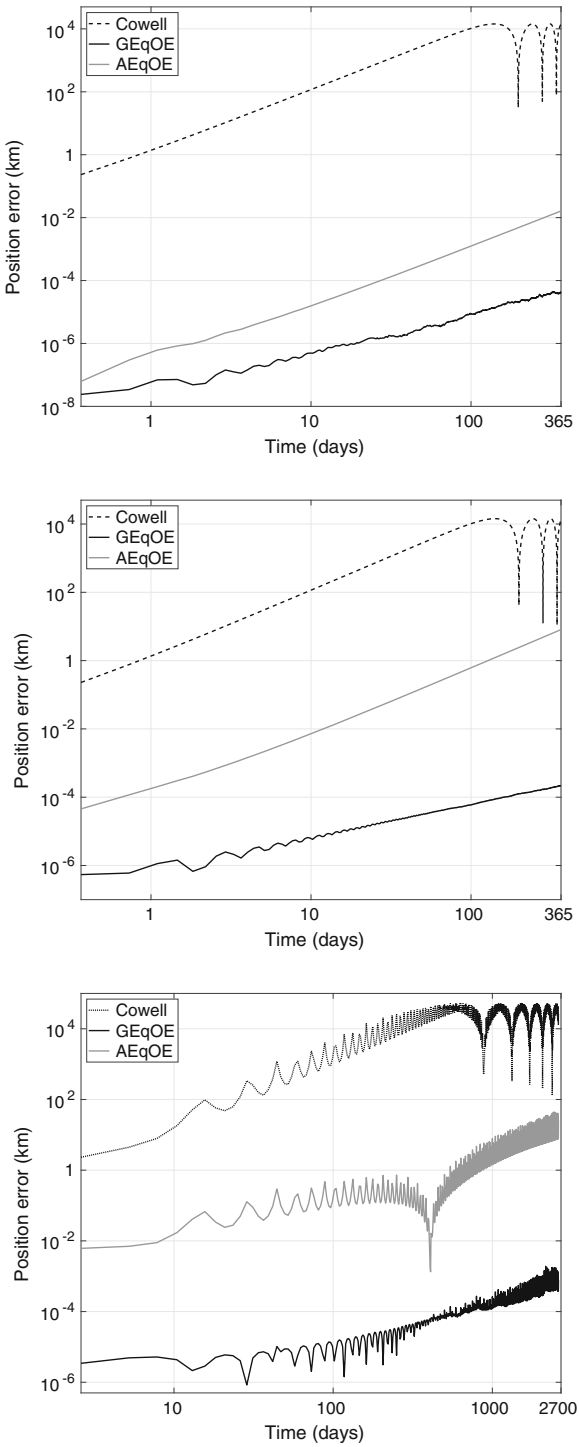

Fig. 6 Time evolution of the position error. The initial conditions are reported in the rows (b), (c), and (d) of Table 1 and correspond to (*top*) a low Earth equatorial orbit, (*middle*) a low Earth polar orbit, and (*bottom*) a Molniya orbit, respectively. The first two orbits are propagated for 365 days, the latter for 2604 days. Perturbations due to the J_2 zonal harmonic of the geopotential and the attraction of the Moon and the Sun are considered. Note that a logarithmic scale is applied to both axes

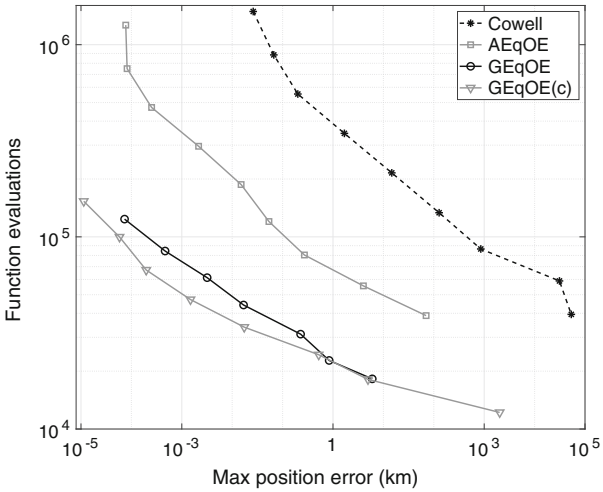

Fig. 7 Function evaluations (see the text) versus maximum position error in 85.6 days of propagation for decreasing (right to left) values of the integrator relative tolerance. The initial conditions correspond to the Molniya orbit reported in the row (d) of Table 1. Perturbations due to the J_2 zonal harmonic of the geopotential and the attraction of the Moon and the Sun are considered. Note that a logarithmic scale is applied to both axes

motion quantities. The new elements are defined for a negative value of the total energy and a positive value of the effective potential energy in (5). They are non-singular for circular and equatorial trajectories and are affected by the same singularities as their classical counterparts (retrograde equatorial and rectilinear orbits). Equations of motions, transformation from and to Cartesian coordinates are provided along with the associated Jacobian matrices.

Representative propagation tests for low Earth orbits show a dramatic increase in performance (accuracy and computational cost) for a propagator based on the new elements compared to the alternate equinoctial orbital elements as well as Cartesian coordinates. Ongoing research is focused on the application of the proposed elements to the problem of uncertainty propagation.

Acknowledgements G. Baù acknowledges the projects MIUR-PRIN 20178CJA2B titled "New frontiers of Celestial Mechanics: theory and applications", and PRA 2020-82 titled "Sistemi dinamici in logica, geometria, fisica matematica e scienza delle costruzioni". Moreover, he acknowledges the INdAM group "Gruppo Nazionale per la Fisica Matematica". The authors acknowledge the reviewers for their useful comments and Alicia Martínez Cacho for checking many equations of this paper. The views expressed are those of the authors and do not necessarily represent the views of ispace, inc.

Declarations

Conflict of Interest The authors declare that they have no conflict of interest.

A Alternative formulation

An alternative set of generalized equinoctial orbital elements is obtained by replacing q_1, q_2 with the Euler parameters e_1, e_2, e_3, e_4 that define the orientation of the equinoctial reference frame Σ_{eq} with respect to Σ (see eq 2):

$$e_1 := \cos\frac{i}{2}\cos\Omega, \quad e_2 := \sin\frac{i}{2}, \quad e_3 := \cos\frac{i}{2}\sin\Omega, \quad e_4 := 0.$$

The Euler parameters allow us to partially control the error accumulation during the propagation by monitoring the quantity $e_1^2 + e_2^2 + e_3^2 + e_4^2$. On the other hand, they make the set of GEqOE redundant, increasing the dimension of the state vector from 6 to 7.

If the Euler parameters e_1, e_2, e_3 are used in place of q_1, q_2, then $\mathbf{e}_X$, $\mathbf{e}_Y$ are computed from the formulae

$$\mathbf{e}_X = \left(e_1^2 + e_2^2 - e_3^2,\ -2e_1e_3,\ 2e_2e_3\right)^T,$$
$$\mathbf{e}_Y = \left(2e_1e_3,\ e_1^2 - e_2^2 - e_3^2,\ -2e_1e_2\right)^T.$$

Moreover, we have

$$\dot{e}_1 = \frac{1}{2}(w_h e_2 + w_X e_3),$$
$$\dot{e}_2 = -\frac{1}{2}(w_h e_1 - w_Y e_3),$$
$$\dot{e}_3 = -\frac{1}{2}(w_X e_1 + w_Y e_2),$$

where w_X, w_Y are obtained as in (52) and

$$w_h = \frac{e_2}{e_1^2 + e_3^2}(e_3 w_X - e_1 w_Y).$$

While the quantities e_1, e_2, e_3 are defined for any inclination, the time derivatives of e_1, e_2 become singular for $i = \pi$.

B Examples of conversion between Cartesian position and velocity coordinates and the GEqOE

The results reported in this section are obtained using MATLAB R2020b.

Consider the four test cases described in Sect. 7 and the corresponding four sets of initial conditions in Table 1. For all of them, the function $\mathscr{U}$ is given in (56). The corresponding values of the GEqOE are shown in Table 3. They are obtained by first computing the Cartesian position and velocity coordinates (see Table 2) and then applying the procedure described in Sect. 3. The constants μ, J_2, r_e used for the transformations are:

$$\begin{aligned} \mu &= 398600.4354360959\,\mathrm{km}^3/\mathrm{s}^2 \\ J_2 &= 1.08262617385222 \times 10^{-3}, \\ r_e &= 6378.1366\,\mathrm{km}. \end{aligned} \tag{59}$$

Next, for a particular example, we show a step-by-step guide to convert to and from GEqOE and Cartesian position and velocity coordinates. The numbers reported below are taken from the output displayed by MATLAB R2020b when the long fixed-decimal format is selected. We used the values given by r_e and $(r_e^3/\mu)^{1/2}$ as units of length and time. With this choice, all the equations in the paper can be applied by replacing μ with 1 and dimensional quantities with the corresponding non-dimensional ones.

Pick the six values of the row labeled by (**a**) in Table 2:

$$x = 7178.1366\,\mathrm{km}, \qquad \dot{x} = 0\,\mathrm{km/s},$$
$$y = 0\,\mathrm{km}, \qquad \dot{y} = 5.269240572916780\,\mathrm{km/s},$$

Table 2 Position (km) and velocity (km/s) coordinates with respect to the J2000 frame computed from the four sets of initial conditions shown in Table 1. Some numbers are rounded off

	x	y	z
(a)	7178.1366	0	0
(b)	7178.1366	0	0
(c)	7178.1366	0	0
(d)	1548.3509	−2681.8225	−6183.9707
	$\dot{x}$	$\dot{y}$	$\dot{z}$
(a)	0	5.2692	5.2692
(b)	0	7.4518	0
(c)	0	0	7.4518
(d)	8.6725	5.0071	0

Table 3 GEqOE computed from the four sets of Cartesian position and velocity coordinates, which correspond to the orbital elements in Table 1. We assumed that $GM = \mu$ in the expression of $\mathscr{U}$ in (56). The values of the quantities ν and $\mathcal{L}$ ($= \mathcal{L}_0$) are in rad/s and rad, respectively. Some numbers are rounded off

	ν	p_1	p_2
(a)	1.0395×10^{-3}	0	-8.5476×10^{-4}
(b)	1.0395×10^{-3}	0	-8.5476×10^{-4}
(c)	1.0395×10^{-3}	0	-8.5476×10^{-4}
(d)	1.4445×10^{-4}	−0.64197	0.37064
	$\mathcal{L}$	q_1	q_2
(a)	0	0	0.41421
(b)	0	0	0
(c)	0	0	1
(d)	−1.0472	0.30881	0.53487

$$z = 0\,\text{km}, \qquad \dot{z} = 5.269240572916780\,\text{km/s}.$$

Following Sect. 3, we get in sequence:

$$\mathbf{e}_r = (1,\ 0,\ 0)^T, \quad \mathbf{e}_f = (0,\ 0.707106781186548,\ 0.707106781186548)^T,$$
$$\mathbf{e}_h = (0,\ -0.707106781186548,\ 0.707106781186548)^T,$$
$$r = 7178.1366\,\text{km}, \quad \dot{r} = 0\,\text{km/s}, \quad h = 53490.26429528814\,\text{km}^2/\text{s},$$
$$\mathscr{U} = -0.023732242207310\,\text{km}^2/\text{s}^2, \quad \mathscr{E} = -27.788628457479671\,\text{km}^2/\text{s}^2,$$
$$\nu = 0.001039460266303\,\text{rad/s},$$
$$q_1 = 0, \quad q_2 = 0.414213562373095,$$
$$\mathbf{e}_X = (1,\ 0,\ 0)^T, \quad \mathbf{e}_Y = (0,\ 0.707106781186547,\ 0.707106781186548)^T,$$
$$c = 53467.39881650716\,\text{km}^2/\text{s},$$
$$\boldsymbol{\upsilon} = (0,\ 5.266988131092099,\ 5.266988131092099)^T\,\text{km/s},$$
$$\mathbf{g} = (-8.547571013161059 \times 10^{-4},\ 0,\ 0)^T,$$
$$p_1 = 0, \quad p_2 = -8.547571013161059 \times 10^{-4},$$
$$X = 7178.1366\,\text{km}, \quad Y = 0\,\text{km},$$

$$
\begin{aligned}
&a = 7172.006276704303\,\text{km}, \quad \alpha = 0.500000091326246,\\
&\sin\mathcal{K} = 0, \quad \cos\mathcal{K} = 1,\\
&\mathcal{L} = 0\,\text{rad}.
\end{aligned}
$$

Then, we convert the values of ν, p_1, p_2, $\mathcal{L}$, q_1, q_2 obtained above to position and velocity. Following Sect. 4, we get in sequence:

$$
\begin{aligned}
&\mathcal{K} = 0\,\text{rad},\\
&\mathbf{e}_X = (1,\ 0,\ 0)^T, \quad \mathbf{e}_Y = (0,\ 0.707106781186547,\ 0.707106781186548)^T,\\
&a = 7172.006276704303\,\text{km}, \quad \alpha = 0.500000091326246,\\
&X = 7178.136600000001\,\text{km}, \quad Y = 0\,\text{km},\\
&\mathbf{r} = (7178.136600000001,\ 0,\ 0)^T\,\text{km},\\
&r = 7178.136600000001\,\text{km}, \quad \dot{r} = 0\,\text{km/s},\\
&\mathscr{U} = -0.023732242207310\,\text{km}^2/\text{s}^2,\\
&c = 53467.39881650716\,\text{km}^2/\text{s}, \quad h = 53490.26429528814\,\text{km}^2/\text{s},\\
&\dot{\mathbf{r}} = (0,\ 5.269240572916779,\ 5.269240572916779)^T\,\text{km/s}.
\end{aligned}
$$

C Further details about Figs. 3, 5, and 7

We report below the *true* positions and velocities at the final epoch of propagation used to obtain the performance plots of Figs. 3, 5, and 7. These vectors are expressed in the J2000 reference frame.

The J_2 value (see eq. 59) of the Earth's gravitational expansion was taken from the EGM2008 model. The ephemerides of the Sun and the Moon and the values of the parameters μ, r_e (see eq 59) were retrieved from the planetary and lunar ephemerides DE430. Moreover, the precession, nutation, and polar motion of the Earth are completely neglected so that the Earth's spin axis is fixed and equal to that of the reference epoch J2000.

We denote by t_0 and t_f the initial and final epochs of propagation.

(*) Fig. 3, t_0 = 2020 Jan 01 00:00:00 UTC, t_f = 2020 Jan 13 00:00:00 UTC:

$$
\begin{aligned}
x_f &= -5398.929377366906\,\text{km}, & \dot{x}_f &= 2.214482567493\,\text{km/s},\\
y_f &= -390.257240638229\,\text{km}, & \dot{y}_f &= -6.845637008953\,\text{km/s},\\
z_f &= -4693.719111636971\,\text{km}, & \dot{z}_f &= -1.977748618717\,\text{km/s}.
\end{aligned}
$$

(*) Fig. 5 (top panel), t_0 = 2020 Jan 01 00:00:00 UTC, t_f = 2020 Jan 13 00:00:00 UTC:

$$
\begin{aligned}
x_f &= -274.761002943290\,\text{km}, & \dot{x}_f &= 7.465328216770\,\text{km/s},\\
y_f &= -7154.555995859508\,\text{km}, & \dot{y}_f &= -0.288082051862\,\text{km/s},\\
z_f &= -0.095489199987\,\text{km}, & \dot{z}_f &= -0.000288808942\,\text{km/s}.
\end{aligned}
$$

(*) Fig. 5 (middle panel), t_0 = 2020 Jan 01 00:00:00 UTC, t_f = 2020 Jan 13 00:00:00 UTC:

$$
\begin{aligned}
x_f &= -6127.562058484711\,\text{km}, & \dot{x}_f &= -3.876493609204\,\text{km/s},\\
y_f &= 0.290815939820\,\text{km}, & \dot{y}_f &= 0.000242489963\,\text{km/s},\\
z_f &= 3725.501491458693\,\text{km}, & \dot{z}_f &= -6.369562182446\,\text{km/s}.
\end{aligned}
$$

(*) Fig. 5 (bottom panel) and Fig. 7, $t_0 = 2020$ Jan 01 00:00:00 UTC, $t_f = 2020$ Mar 26 14:27:30 UTC:

$$\begin{aligned} x_f &= 10732.86105177698\,\text{km}, & \dot{x}_f &= 3.96389903452\,\text{km/s}, \\ y_f &= 2632.59989195335\,\text{km}, & \dot{y}_f &= 3.86270637636\,\text{km/s}, \\ z_f &= -1133.57673525621\,\text{km}, & \dot{z}_f &= 5.12156998778\,\text{km/s}. \end{aligned}$$

D Derivation of eqs (38), (39), and (42)

We set the right-hand sides of (31), (32) equal to the right-hand sides of (33), (34), respectively. By solving the resulting equations for $\cos L$, $\sin L$ and taking into account (19), (20), (22), (40), we find

$$\begin{aligned} \cos L &= \frac{a}{r}\left[\alpha p_1 p_2 \sin\mathcal{K} + (1-\alpha p_1^2)\cos\mathcal{K} - p_2\right], \\ \sin L &= \frac{a}{r}\left[\alpha p_1 p_2 \cos\mathcal{K} + (1-\alpha p_2^2)\sin\mathcal{K} - p_1\right]. \end{aligned} \tag{60}$$

Noting that

$$X = r\cos L, \qquad Y = r\sin L, \tag{61}$$

we obtain (42).

System (60) can be solved for $\cos\mathcal{K}$, $\sin\mathcal{K}$ to yield relations (39). By inserting the expressions given in (39) in the generalized Kepler's equation (30), we have

$$\mathcal{L} = \mathcal{K} + \frac{1}{a\beta}(Xp_1 - Yp_2),$$

which corresponds to (38).

E Time derivatives of p_1, p_2

From equations (17), (18), we have

$$\dot{p}_1 = \dot{g}\sin\Psi + g\dot{\Psi}\cos\Psi, \tag{62}$$

$$\dot{p}_2 = \dot{g}\cos\Psi - g\dot{\Psi}\sin\Psi. \tag{63}$$

For the time derivative of g, we use relation (9) and so we need the expressions of $\dot{\mathscr{E}}$, $\dot{c}$. The former is given in (46), the latter, which is derived from the definition of c provided in (6), results:

$$\dot{c} = \frac{1}{c}[r^2\dot{\mathscr{E}} + r\dot{r}(2\mathscr{U} - rF_r)]. \tag{64}$$

Then, we find

$$\dot{g} = \frac{1}{\mu^2 g}\left[(c^2 + 2\mathscr{E}r^2)\dot{\mathscr{E}} + 2\mathscr{E}r\dot{r}(2\mathscr{U} - rF_r)\right].$$

After writing $2\mathscr{E}$ as a function of c and g by means of (9), and using

$$r = \frac{c^2}{\mu(1+g\cos\theta)}, \qquad \dot{r} = \frac{\mu}{c}g\sin\theta,$$

which directly follows from (11), (12), we obtain

$$\dot{g} = \frac{r}{\mu}(\tilde{\varsigma}\cos\theta + \varsigma g)\dot{\mathscr{E}} + \frac{g^2-1}{c}\varsigma\sin\theta(2\mathscr{U} - rF_r), \tag{65}$$

where ς, $\tilde{\varsigma}$ are given by

$$\varsigma = \frac{\mu r}{c^2}, \qquad \tilde{\varsigma} = 1 + \varsigma.$$

From the definition of Ψ, we write

$$g\dot{\Psi} = g\dot{L} - g\dot{\theta}. \tag{66}$$

The expression of $\dot{L}$ can be derived, for example, from Battin (1999, eqs. 10.78, 10.81, pp. 500–501):

$$\dot{L} = \frac{h}{r^2} + \frac{r}{h}F_h\tan\frac{i}{2}\sin(\omega + f). \tag{67}$$

The time derivative of θ is obtained by differentiation of both sides of equation

$$\tan\theta = \frac{r\dot{r}c}{c^2 - \mu r},$$

which is a consequence of (11), (12). We first use

$$\ddot{r} = -\frac{\mu}{r^2} + \frac{c^2}{r^3} - \frac{2\mathscr{U}}{r} + F_r, \tag{68}$$

to get

$$\dot{\theta} = \frac{c}{r^2} - \frac{c}{\mu r g}[(2\mathscr{U} - rF_r)\cos\theta + \tilde{\varsigma}\dot{c}\sin\theta].$$

Then, we replace $\dot{c}$ with the expression in (64) and find

$$\dot{\theta} = \frac{c}{r^2} - \frac{1}{\mu g}\left[(\tilde{\varsigma} r\sin\theta)\dot{\mathscr{E}} + \left(\frac{c}{r}\cos\theta + \tilde{\varsigma}\dot{r}\sin\theta\right)(2\mathscr{U} - rF_r)\right]. \tag{69}$$

From equations (66), (67), (69), we have

$$g\dot{\Psi} = \frac{g}{r^2}(h - c) - g w_h + \frac{\tilde{\varsigma} r}{\mu}\dot{\mathscr{E}}\sin\theta + \frac{1}{c}(\tilde{\varsigma} g + \varsigma\cos\theta)(2\mathscr{U} - rF_r), \tag{70}$$

where we used the definition of w_h in (14) and made the substitution

$$\frac{c}{r}\cos\theta + \tilde{\varsigma}\dot{r}\sin\theta = \frac{\mu}{c}(\tilde{\varsigma} g + \varsigma\cos\theta).$$

The expressions of $\dot{g}$, $g\dot{\Psi}$, given in (65), (70), are plugged in (62), (63), and by considering the definitions of p_1, p_2 (see 17, 18) and the relation $L = \Psi + \theta$, we get

$$\dot{p}_1 = p_2\left(\frac{h-c}{r^2} - w_h\right) + \frac{1}{c}\left(\frac{r\dot{r}}{c}p_1 + \tilde{\varsigma}p_2 + \varsigma\cos L\right)(2\mathscr{U} - rF_r) + \frac{r}{\mu}(\varsigma\, p_1 + \tilde{\varsigma}\sin L)\dot{\mathscr{E}},$$

$$\dot{p}_2 = p_1\left(w_h - \frac{h-c}{r^2}\right) + \frac{1}{c}\left(\frac{r\dot{r}}{c}p_2 - \tilde{\varsigma}p_1 - \varsigma\sin L\right)(2\mathscr{U} - rF_r) + \frac{r}{\mu}(\varsigma\, p_2 + \tilde{\varsigma}\cos L)\dot{\mathscr{E}}.$$

Finally, in the two equations above we note that

$$\frac{r\dot{r}}{c}p_1 + \tilde{\varsigma}p_2 + \varsigma\cos L = \frac{r}{a}\cos L + 2p_2,$$

$$\frac{r\dot{r}}{c}p_2 - \tilde{\varsigma}p_1 - \varsigma \sin L = -\frac{r}{a}\sin L - 2p_1,$$

where we used (33), (34).

F Time derivative of $\mathcal{L}$

From equations (30) and (31), we have

$$\dot{\mathcal{L}} = \dot{\mathcal{K}}\frac{r}{a} + \dot{p}_1 \cos \mathcal{K} - \dot{p}_2 \sin \mathcal{K}, \tag{71}$$

Let us first deal with the term $\dot{p}_1 \cos \mathcal{K} - \dot{p}_2 \sin \mathcal{K}$. Using relations (42) for X, Y in the expressions of $\dot{p}_1$, $\dot{p}_2$ given in (47), (48), and then considering (31), (32), we get

$$\begin{aligned}\dot{p}_1 \cos \mathcal{K} - \dot{p}_2 \sin \mathcal{K} = &\left(\frac{h-c}{r^2} - w_h\right)\left(1 - \frac{r}{a}\right) + \frac{1}{c}\left[2 - \frac{r}{a} - \alpha\frac{(r\dot{r})^2}{\mu a}\right](2\mathscr{U} - rF_r)\\ &+ \frac{r\dot{r}\alpha}{\mu c}\left[\varrho + r\left(\frac{1}{\alpha} - \frac{r}{a}\right)\right]\dot{\mathscr{E}},\end{aligned} \tag{72}$$

where α, β are defined in (40), and

$$w = \sqrt{\frac{\mu}{a}}.$$

We compute now the time derivative of $\mathcal{K}$. From (15), (29), we have

$$\dot{\mathcal{K}} = \dot{L} + \dot{G} - \dot{\theta}. \tag{73}$$

The expressions of $\dot{L}, \dot{\theta}$ are written in (67), (69). By differentiation of both sides of equation

$$\tan G = \frac{r\dot{r}}{w(a-r)},$$

which follows from (24), (25), and using (68), we find

$$\dot{G} = \frac{w}{r} - \frac{1}{gwa}\left[\frac{\mu r \sin\theta}{2ca^2}(r+a)\dot{a} + (\cos G)(2\mathscr{U} - rF_r)\right].$$

Then, considering that

$$\cos G = \frac{\cos\theta + g}{1 + g\cos\theta}, \qquad \dot{a} = \frac{2a^2}{\mu}\dot{\mathscr{E}},$$

we can write

$$\dot{G} = \frac{w}{r} - \frac{r}{cgwa}\left[\sin\theta(r+a)\dot{\mathscr{E}} + \frac{\mu}{c}(\cos\theta + g)(2\mathscr{U} - rF_r)\right]. \tag{74}$$

From equations (73) and (67), (69), (74), we obtain

$$\dot{\mathcal{K}} = \frac{w}{r} + \frac{h-c}{r^2} - w_h + \frac{1}{c}\left[1 + \alpha\left(1 - \frac{r}{a}\right)\right](2\mathscr{U} - F_r r) - \frac{r\dot{r}\alpha}{\mu w}\left(1 - \frac{r}{a\beta}\right)\dot{\mathscr{E}}. \tag{75}$$

Finally, by making the substitutions

$$\dot{r}^2 = -\frac{\mu}{a} + \frac{2\mu}{r} - \frac{c^2}{r^2}, \qquad 1 - \frac{r}{a\beta} = 1 - \beta\varsigma,$$

in equations (72), (75), respectively, and taking into account the relation $\alpha\beta = 1 - \alpha$, we find from equation (71) the expression of $\dot{\mathcal{L}}$ reported in (49).

References

Aristoff, J.M., Horwood, J.T., Alfriend, K.T.: On a set of J_2 equinoctial orbital elements and their use for uncertainty propagation. Celest. Mech. Dyn. Astron. **133**(3), 1–19 (2021)

Arsenault, J.L., Ford, K.C., Koskela, P.E.: Orbit determination using analytic partial derivatives of perturbed motion. AIAA J. **8**(1), 4–9 (1970)

Battin, R.H.: An Introduction to the Mathematics and Methods of Astrodynamics, revised AIAA Education Series, AIAA, Reston, VA (1999)

Baù, G., Bombardelli, C.: Time elements for enhanced performance of the Dromo orbit propagator. Astron. J. **148**(43), 1–15 (2014)

Baù, G., Bombardelli, C., Peláez, J.: A new set of integrals of motion to propagate the perturbed two-body problem. Celest. Mech. Dyn. Astron. **116**(1), 53–78 (2013)

Baù, G., Bombardelli, C., Peláez, J., Lorenzini, E.: Non-singular orbital elements for special perturbations in the two-body problem. Mon. Not. R. Astron. Soc. **454**(3), 2890–2908 (2015)

Biria, A.D., Russell, R.P.: Equinoctial elements for Vinti theory: generalizations to an oblate spheroidal geometry. Acta Astronaut. **153**, 274–288 (2018)

Biria, A.D., Russell, R.P.: Analytical solution to the vinti problem in oblate spheroidal equinoctial orbital elements. J. Astronaut. Sci. **67**(1), 1–27 (2020)

Broucke, R.A.: On the matrizant of the two-body problem. Astron. Astrophys. **6**, 173–182 (1970)

Broucke, R.A., Cefola, P.J.: On the equinoctial orbit elements. Celest. Mech. **5**(3), 303–310 (1972)

Cefola, P.J.: Equinoctial orbit elements – application to artificial satellite orbits. In: AIAA/AAS Astrodynamics Conference, AIAA paper 72–937 (1972)

Danielson, D.A., Sagovac, C.P., Neta, B., Early, L.W.: Semianalytic satellite theory. Tech. Rep. NPS-MA-95-002, Naval Postgraduate School, Monterey, CA (1995)

Dormand, J.R., Prince, P.J.: A family of embedded Runge-Kutta formulae. J. Comput. Appl. Math. **6**(1), 19–26 (1980)

Goldstein, H.: Classical mechanics, 2nd edn. Addison-Wesley, Reston, VA (1980)

Horwood, J.T., Aragon, N.D., Poore, A.B.: Gaussian sum filters for space surveillance: theory and simulations. J. Guid. Control. Dyn. **34**(6), 1839–1851 (2011)

Junkins, J.L., Akella, M.R., Alfriend, K.T.: Non-gaussian error propagation in orbital mechanics. In: Advances in the Astronautical Sciences, 283–298 (1996)

Kéchichian, J.A.: Applied nonsingular astrodynamics. Cambridge University Press, Optimal Low-Thrust Orbi Transfer (2018)

Lagrange, J.L.: Théorie des variations séculaires del éléments des planètes. Première partie contenant les principes et les formules générales pour déterminer ces variations. Nouveaux mémoires de l'Académie des Sciences et Belles-Lettres de Berlin Reprinted in Œuvres de Lagrange, Gauthier-Villars, Paris (1870), **5**, pp. 125–207 (1781)

Milani, A., Gronchi, G.F.: Theory of orbit determination. Cambridge University Press, Cambridge, UK (2010)

Stiefel, E.L., Scheifele, G.: Linear and regular celestial mechanics. Springer-Verlag, Berlin (1971)

Vinti, J.P.: New method of solution for unretarded satellite orbits. J. Res. Nat. Bureau of Stand-B Math. Math. Phys. **62B**(2), 105–116 (1959)

Walker, M.J.H., Ireland, B., Owens, J.: A set of modified equinoctial orbit elements. Celest. Mech. **36**(4), 409–419 (1985)